Lensing Systematics from Space: Modeling PSF effects in the SNAP survey

H. F. Stabenau[†], B. Jain[†], G. Bernstein[†], M. Lampton[‡]

[†] Dept. of Physics and Astronomy, University of Pennsylvania, Philadelphia, PA

[‡] Lawrence Berkeley National Laboratory, Berkeley, CA

hstabena, bjain, garyb@physics.upenn.edu, mlampton@ssl.berkeley.edu

Received _____; accepted _____

ABSTRACT

Anisotropy in the point spread function (PSF) contributes a systematic error to weak lensing measurements. In this study we use a ray tracer that incorporates all the optical elements of the SNAP telescope to estimate this effect. Misalignments in the optics generates PSF anisotropy, which we characterize by its ellipticity. The effect of three time varying effects: thermal drift, guider jitter, and structural vibration on the PSF are estimated for expected parameters of the SNAP telescope. Multiple realizations of a thousand square degree mock survey are then generated to include the systematic error pattern induced by these effects. We quantify their contribution to the power spectrum of the lensing shear. We find that the dominant effect comes from the thermal drift, which peaks at angular wavenumbers $l \sim 10^3$, but its amplitude is over one order of magnitude smaller than the size of the expected statistical error. While there are significant uncertainties in our modeling, our study indicates that time-varying PSFs will contribute at a smaller level than statistical errors in SNAP's weak lensing measurements.

1. Introduction

Current measurements of cosmic shear in the literature have systematic errors at or below the $\lesssim 10\%$ level, most likely generated by insufficiently corrected optical and atmospheric distortions. Given the accuracy requirements for the shear (between 0.1-1%) for the SNAP survey (Aldering et al. 2004; Albert et al. 2004), it is clear that progress on the optical distortions and shape measurement techniques is essential. The PSF may have spatial and temporal variations and is sampled at only the locations of stars, from where it must be interpolated onto the galaxies. If each exposure had many stars distributed

around the image, then we wouldn't have to worry about time variations in the PSF since there would be enough information in each exposure to subtract the PSF. If the usable star density is too low however, subtracting a single static PSF from every exposure will be inadequate. Recent work shows that the many exposures used in the planned SNAP survey could be used to make this correction very precisely (Jarvis & Jain 2004). In this paper, we estimate the shear power spectra for a fully dynamic treatment of the observatory with thermal and mechanical PSF disturbances that continue throughout the one year survey. To model a first-order PSF correction, we use an imperfect static PSF that is held fixed throughout the same one year survey. A further improvement not pursued here would be to update the PSF model throughout the survey using daily field star images. Our shear power spectra should therefore be regarded as upper limits to the corrected shear spectra, given the model parameters we have assumed.

An estimate of the limiting systematics for ground- and space-based WL data requires some knowledge of the amplitude and variability of the PSF. We are working with other members of the SNAP Weak Lensing Working Group (WLWG), and the SNAP optical-mechanical engineers, to model the temporal behavior of its PSF. In this section we describe our work on systematic errors: calculation of the expected instrumental distortion for SNAP by modeling the dominant sources of PSF anisotropy.

PSF anisotropy and time variation have been the dominant systematic errors in most lensing measurements (Refregier 2003). This is one reason why a space instrument is expected to be superior for lensing. The expected variations, *e.g.* thermal effects, should be very slow, given the absence of gravity and the nearly constant thermal environment. It is therefore important to quantify the time rate of change of the PSF for a nominal SNAP mission to determine the degree to which the recovered shear maps can be corrected for instrumental effects. An initial assessment of the SNAP PSF time variations was presented

by Sholl et al. (2005).

2. PSF of the SNAP telescope

We have calculated the PSF ellipticity on a grid over the field of view of the instrument, subject to specified optical misalignment parameters. The first step is to use a ray-tracing telescope simulator for SNAP to generate monochromatic PSF images at one micron wavelength as a function of position of the field of view and telescope misalignment. The ray tracer filled the aperture with a grid of rays from a distant point source, propagating them through the optical system to evaluate the pupil's complex transmission, and then Fourier transforming and squaring to get the image irradiance. Finally, we determined the second moments of the image and from them its ellipticity components.

The resulting pattern of PSF anisotropy on the focal plane for a sample misalignment is shown in Figure 1. The length and orientation of each whisker represents the magnitude and orientation of the ellipticity at that position. The typical ellipticity shown is $\sim 0.2\%$. We define the ellipticity in terms of the second moments of the diffracted light,

$$\begin{aligned} e_1 &= \frac{\mathrm{I_{xx}} - \mathrm{I_{yy}}}{\mathrm{I_{xx}} + \mathrm{I_{yy}}} \\ e_2 &= \frac{2\mathrm{I_{xy}}}{\mathrm{I_{xx}} + \mathrm{I_{yy}}}. \end{aligned}$$

The second moments $\mathrm{I_{ab}}$ for $a, b \in \{\mathrm{x}, \mathrm{y}\}$ are defined as

$$\mathrm{I_{ab}} = \frac{\sum_j I_j a_j b_j}{\sum_j I_j},$$

where I_j are the intensity values of the image pixels, and x_j, y_j are the coordinates of a pixel on the focal plane. The second moments $\mathrm{I_{xx}}$ etc. were computed on an unweighted basis for this study. Applying a weighting kernel appropriate for individual galaxy sizes would slightly reduce our moments but not significantly influence our conclusions. Whiskers

are plotted at an angle of

$$\theta = \frac{1}{2} \arctan \frac{e_2}{e_1}$$

with respect to the x-axis, so that

- pure positive e_1 corresponds to a horizontal whisker (–)
- pure negative e_1 corresponds to a vertical whisker (|)
- pure positive e_2 corresponds to a 45 deg whisker (/)
- pure negative e_2 corresponds to a 45 deg whisker (\)

We next consider the process of generating a survey with SNAP, including effects that cause the PSF ellipticity pattern to change over the length of the survey. This could happen if there were some time-varying instrumental effects, which would translate into a systematically changing PSF across the field of the survey. We modeled a step and repoint survey by taking an exposure using the chips for one filter band, regenerating the PSF, moving the telescope by one CCD chip width, and repeating the process, resulting in a series of strips that we then put together to form a 32×32 square degree mock survey. Multiple realizations of this survey were used to compute the power spectrum.

We considered three time-varying misalignment effects when generating the survey, categorized by the timescale of their variation:

- Thermal drift, which has a timescale of days to weeks;
- Telescope structural vibration, which has a timescale of an hour; and
- Telescope guide jitter, which is different for every exposure.

Of these three effects, the thermal drift effect dominates the time-varying component of the PSF, while the effect of telescope guide jitter turned out to have almost no measurable contribution. The thermal contributions to the PSF include a daily heat pulse from daily attitude maneuvers for telemetry, plus long term drifts from slow changes in the solar longitude and from control system drift. We ignore the daily environmental component because the thermal response is dominated by the thermal control loop on this time scale. We attempted to measure the slower thermal drift contribution to the PSF power spectrum model by modeling a drift in the control system of the sensors that measure the temperature of the struts that hold up the secondary mirror, which undergo thermal expansion and contraction. If the struts have varying lengths, the secondary mirror will be defocussed, decentered, and tilted.

The SNAP focal plane includes dedicated star tracker image sensors to determine the instantaneous attitude (Secroun et al. 2002). By analyzing the positions of stars within an image and comparing to catalogs, the pointing of the telescope is established and corrected via a feedback mechanism with telescope orientation controls. However Poisson noise makes the centroids of stars in the image appear to shift around. The attitude control system responds to this centroid jitter according to its control bandwidth, which cannot be zero. We modelled the jitter by assuming a continuing stream of star centroid information from the star guiders, furnished at a rate of 10 frames/second, with an individual centroid RMS noise level of 1 milliarcsecond per axis, as described by Secroun et al. (2002). Because these successive centroid determinations are based on independent photon arrivals, the deviations will be statistically independent and circularly symmetric around the true long term mean. We assume that the spacecraft attitude control bandwidth is of the order of 0.1 Hz, so that ~ 100 frames are averaged in establishing each attitude, and the RMS jitter in each axis will be reduced tenfold from the individual frame centroids, to ~ 0.1 milliarcsecond. The guider's effect on the PSF turned out to be much smaller than both

Source	Amplitude	Angular scale
thermal decentering along x, y directions	0.8μm	7 milliarcsec
thermal defocus along z direction	0.5μm	4.6 milliarcsec
vibrational tilt	1.6μm	16 milliarcsec
guide jitter	0.01μm	0.1 milliarcsec.

Table 1: Comparison of the RMS widths of the Gaussian distributions from which the misalignment parameters are chosen during the simulated survey.

the vibrational and thermal effects.

Vibrational modes are excited in the structure of the telescope by the vibration of four flywheels that store angular momentum used to rotate the satellite in space. This causes the secondary mirror to vibrate with an amplitude which changes as the flywheel goes in and out of resonance with the telescope structure. We model the vibration effect as the sum of two tilted orientations of the secondary mirror, since the structural vibration modes of the SNAP observatory have frequencies above 15 Hz, and WL exposures have durations of greater than 300 seconds, the number of vibration cycles in each exposure is large, > 4500, allowing us to average the PSF over many cycles. First, we choose an amplitude for the vibration from a Gaussian distribution. Next, we generate two exposures each with the secondary mirror tilted by plus and minus this amplitude. Finally, we average the images from the two orientations. The result is an exposure affected by our model vibrational PSF.

Spacecraft systems engineers provided projections of the magnitude of the thermal and vibrational effects (Ericsson & Stoneking 2001). In order to simulate surveys affected by time-varying misalignments, during each model survey new misalignment parameters for the secondary were chosen from Gaussian distributions every two weeks during the model surveys. The widths of the Gaussian distributions used for the misalignments of the secondary are shown in Table 1.

At intermediate times the misalignments are linearly interpolated between the old and new values. One such realization of the set of model surveys can be seen in Figure 2. The RMS shear in that figure is about 0.1%.

3. Shear Power Spectrum

The systematic error contribution to the lensing shear power spectrum can be obtained by Fourier transforming of the gridded PSF ellipticity maps described above. The power spectrum due to the thermal drift is shown in Figure 4, along with the power spectrum due to vibrations, which has a much smaller amplitude. The power spectrum due to jitter is smaller still, and is below the scale plotted. For the thermal drift, the full contribution to the power spectrum, and the smaller contribution due the residual shear after the static pattern is subtracted are shown. This subtraction is important; for real data it is expected that the static PSF can be measured accurately by interpolating from stars in the image (Jarvis & Jain 2004).

In order to compare the effects of PSF anisotropy with the lensing signal, we generated some simulated shear fields via ray-tracing through N-body simulation boxes (Heitmann et al. 2004). The simulations were performed in a ΛCDM cosmology with a comoving box size of 500 h^{-1}Mpc, and the sources were set at a redshift of $z = 2$. Figure 3 shows a whisker plot of one of the realizations; the RMS shear in the field shown is about 2%. Figure 4 shows that the power spectrum of the time-varying residual of the PSF is typically smaller than the lensing signal by three to four orders of magnitude. It is also much smaller than the statistical errors expected for a thousand square degree survey, also shown in the plot. These include sample variance and the shot noise contribution of galaxies with an RMS ellipticity of $\sigma_\epsilon = 0.4$ (both components combined) and number density $n_g = 100$ per square arcminute. Thus for the standard parameters of the telescope,

we have shown that the power spectrum of the residual error due to PSF anisotropy makes a negligible contribution to the lensing power spectrum.

4. Discussion

We have estimated the effect of three time varying components of PSF anisotropy to the weak lensing power spectrum for the optical design of the SNAP telescope. The time variation of the three effects considered, thermal drift, guider jitter and structural vibrations, leads to spatial patterns in the shear maps inferred from the measured ellipticities of galaxies. We find that for the current best estimates of the amplitude of these three effects, the contribution to the lensing power spectrum is much smaller than the expected statistical errors (after subtracting the static component of the PSF pattern). The systematic error contribution due to PSF anisotropy is therefore negligible, excluding catastrophic failures, revised estimates of the effects we have modeled, or other effects not included in this study.

It would further be of interest to compute the bispectrum of the PSF pattern and compare it to the signal for different triangle configurations. The bispectrum carries important cosmological information, so it is important to test how it will be affected by systematic errors. Preliminary results for special configurations suggest that the contribution to the bispectrum is also much smaller than the expected signal. We will further include worst-case sources of misalignment and catastrophic events such as an extended power outage. Finally, we note that even in the presence of large systematic errors, the estimate of cosmological parameters may be compromised only to a limited extent, as the lensing signal for multiple auto and cross-spectra will in general scale differently with these parameters (Huterer et al. 2006).

We thank Katrin Heitmann, Salman Habib, and Derek Dolney for help with N-body simulation data. We acknowledge useful suggestions from Mike Sholl, Michael Levi, and Saul Perlmutter.

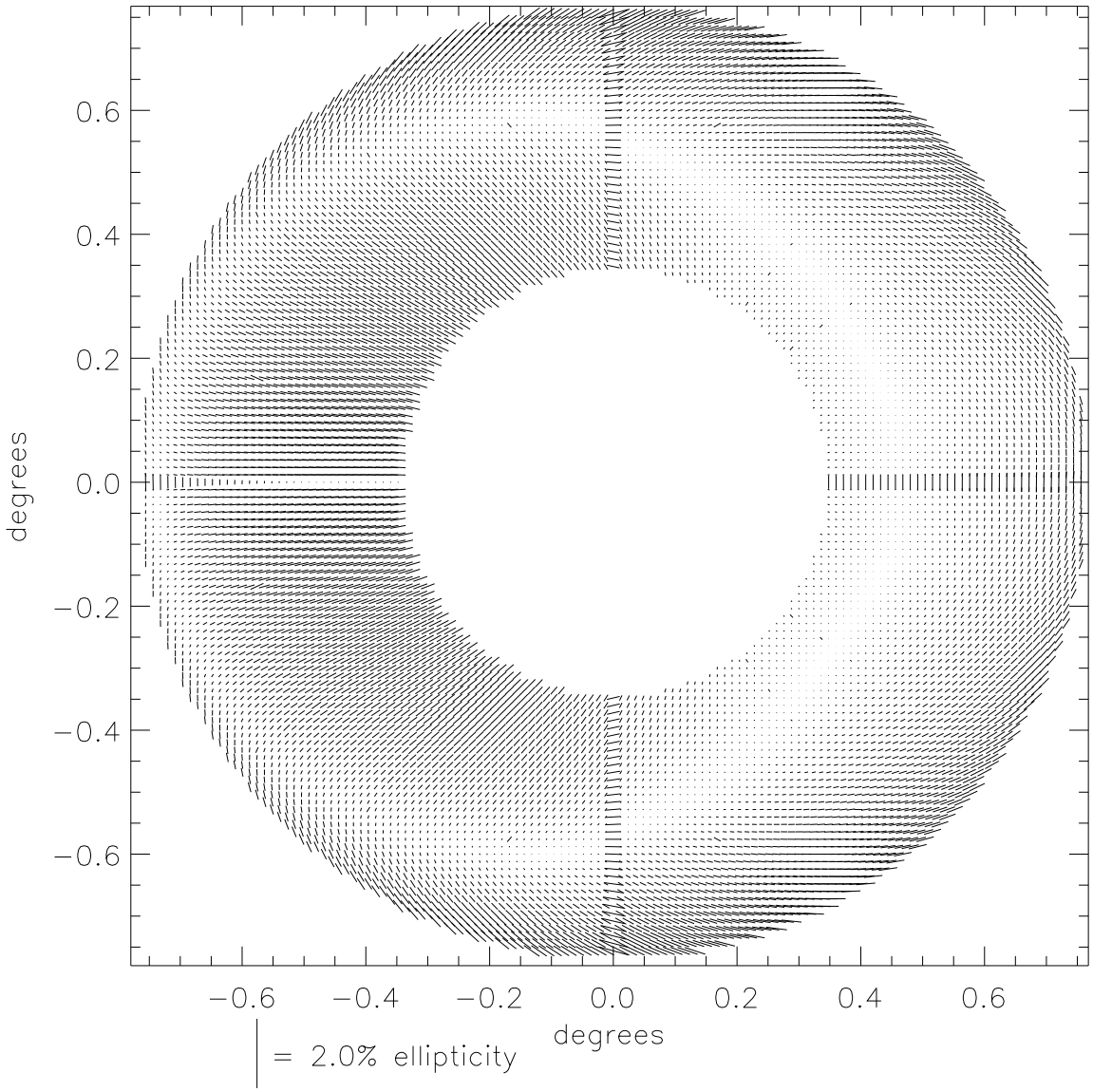

Fig. 1.— Anisotropy in the point spread function (PSF) in the SNAP focal plane. Possible misalignments in the telescope optics have been modeled by ray tracing. In this figure we have modeled a large misalignment: the secondary mirror is off-center by 10μm. The PSF at each position is obtained by computing the second moment of the intensity. The RMS size of the whiskers shown represents a 0.2% ellipticity.

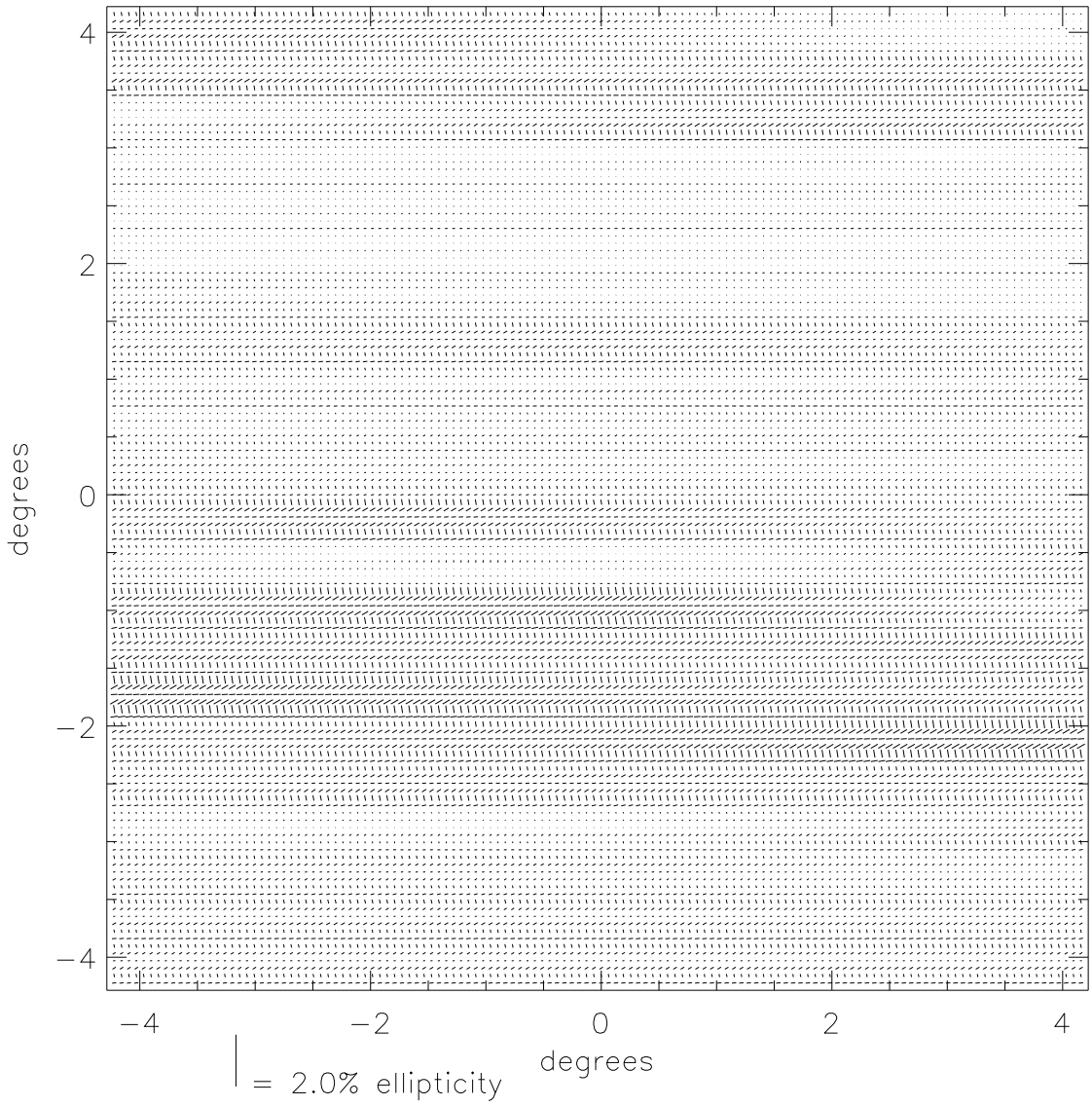

Fig. 2.— PSF anisotropy generated by thermal drift in the SNAP telescope. By choosing misalignment parameters from a Gaussian distribution every two weeks, we obtain a spatially varying PSF pattern with a characteristic length scale. The whiskers in this plot have an RMS ellipticity at the $\sim 0.1\%$ level. Compare with Figure 3, which contains simulated weak lensing whiskers, and Figure 4, which plots the power spectra. Subtracting off the static pattern produces residuals that are smaller by about an order of magnitude, as shown in Figure 4 for the power spectrum.

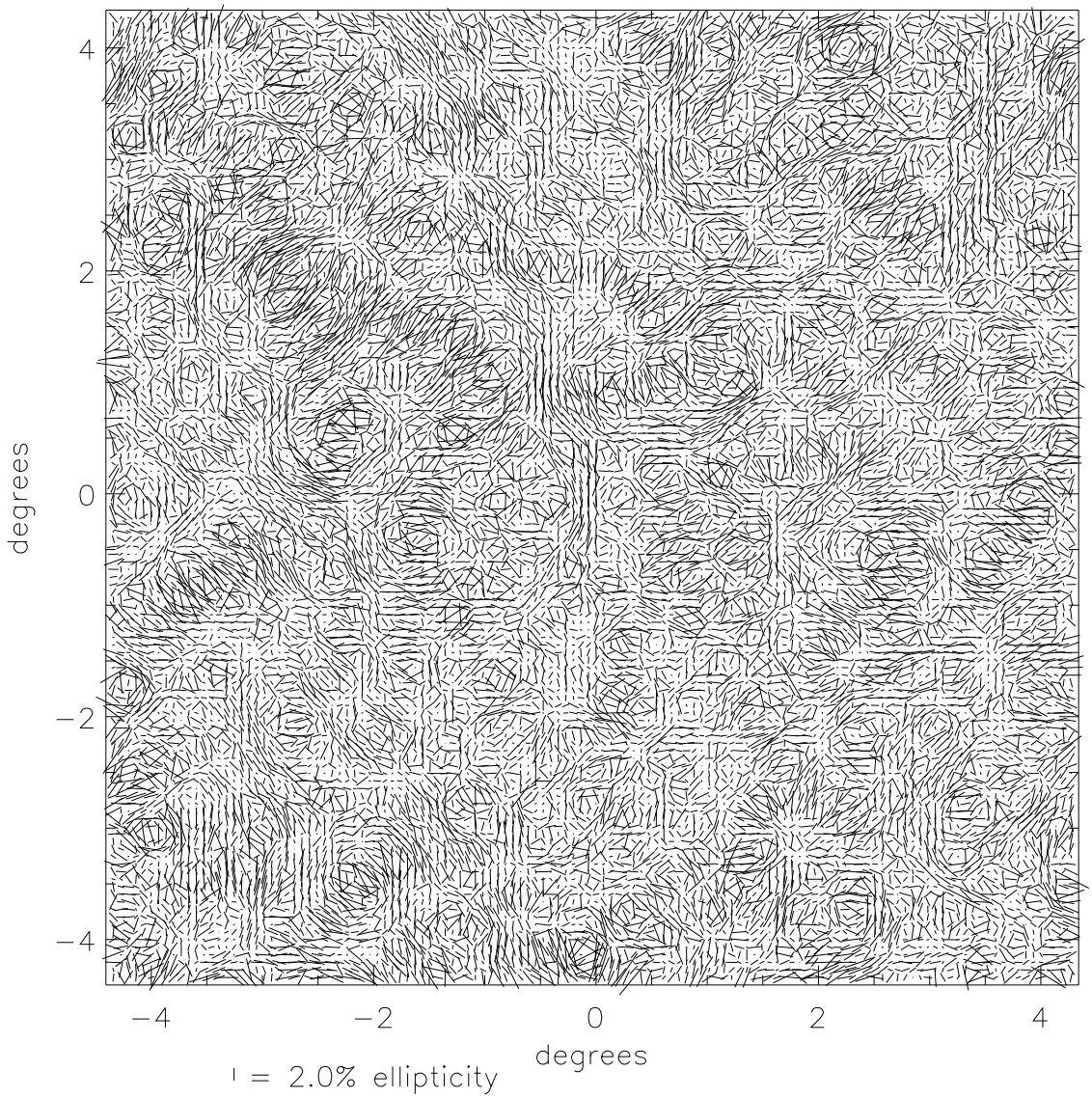

Fig. 3.— Ray-tracing through N-body simulation data provides a way to estimate the importance of the time-varying SNAP PSF. The power spectrum of the ensemble of simulations is the green curve in Figure 4.

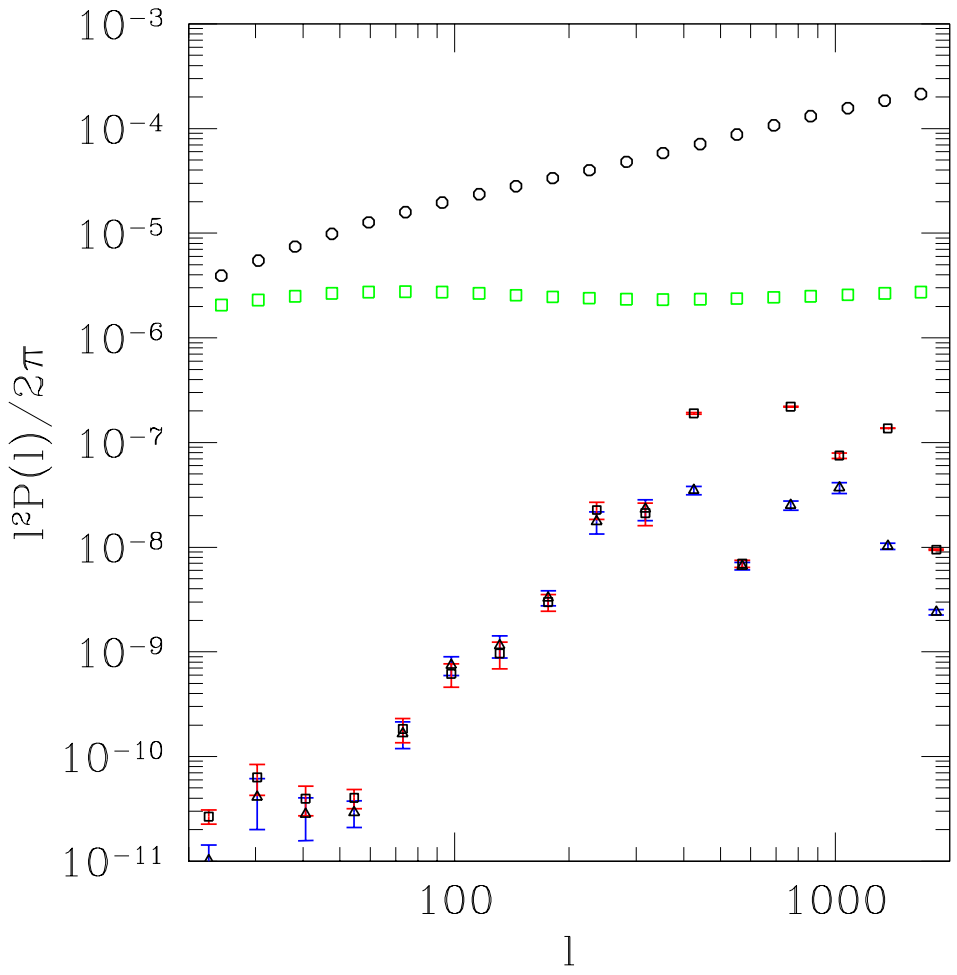

Fig. 4.— Power spectra of the lensing signal and expected PSF anisotropy contamination for the SNAP telescope. Thermal effects and vibration in the structure of the telescope lead to time variation in the PSF anisotropy. This residual power would lead to an additive systematic error in the lensing measurement. Subtracting the static pattern (see text) potentially provides a reduction in PSF power of as much as an order of magnitude. The red curve (squares) is the time-varying power due to thermal effects, and has not had the static PSF pattern subtracted off, whereas the blue curve (triangles) is the residual power after the time invariant pattern is subtracted (as it is expected to be measured accurately). The statistical errors for a 1000 square degree survey are shown by the green squares, along with the power spectrum amplitude of the shear signal from simulations (circles). The statistical error is projected to be larger by > 1 orders of magnitude than the time-varying residual PSF signal. The much smaller residual power from structural vibrations is about two orders of magnitude below the bottom of the plot.

REFERENCES

Aldering, G., et al.: PASP, submitted, astro-ph/0405232 (2004)

Ericsson, A., Stoneking, E.: NASA IMDC Report for SNAP, June 25–28, Chart 12 (2001)

Heitmann, K., Ricker, P. M., Warren, M. S., Habib, S.: Astrophys. J. Suppl. 160, 28 (2005)

Huterer, D., Takada, M., Bernstein, G., Jain, B.: MNRAS 366, 101 (2006)

Jarvis, M., Jain, B., ApJ, submitted, astro-ph/0412234 (2004)

Refregier, A.: ARA&A 41, 645–68 (2003)

J. Albert et al. [SNAP Collaboration]: Astropart. Phys. 20, 377 (2004)

Secroun, A. et al.: Experimental Astronomy 12 (2) 69–85 (2001).

Sholl, M. et al.: Proc. SPIE v.5899 27–38 (2005).